International Journal of Research in Advent Technology, Vol.7, No.3, March 2019
E-ISSN: 2321-9637
Available online at www.ijrat.org

Effect of Transverse Surface Roughness on the Performance of a Magnetic Fluid Based Two Layered Porous Inclined Slider Bearing

R. M. Patel[1], G. M. Deheri[2], Lakshmi S. Desai[3] and. P. A. Vadher[4]
[1]*Department of Mathematics, Gujarat Arts and Science College, Ahmedabad - 380 006 Gujarat State, India*
[2]*Department of Mathematics, Sardar Patel University, Vallabh Vidyanagar 388 120, Gujarat State, India.*
[3]*Department of Mathematics, Faculty of Technology, Dharmsinh Desai University, Nadiad - 387 001, Gujarat, India.*
[4]*Department of Physics, Government Science College, Gandhinagar - 382 016 Gujarat State, India.*
[1] *Corresponding author: rmpatel2711@gmail.com*

Abstract-Efforts have been made to analyze the performance of two layered porous inclined slider bearing with transversely rough surfaces under the presence of a magnetic fluid lubricant. The external applied magnetic field is oblique to the lower surface. The surface roughness is characterized by a stochastic random variable with non-zero mean, variance and skewness. The associated stochastically averaged Reynolds' equation is solved to obtain the pressure distribution leading to the calculation of load carrying capacity. Further, the expression for friction is derived and the position of centre of pressure has been determined. The computed results show that the bearing system registers a relatively better performance as compared to that of a bearing system dealing with a conventional lubricant. The transverse surface roughness induces an adverse effect on the steady state performance. Besides, providing an additional degree of freedom, this investigation offers some scopes for reducing the adverse effect of porosity and standard deviation by the positive effect of magnetization in the case of negatively skewed roughness when negative variance is involved. This investigation conclusively establishes that the porosity parameter plays a crucial role from design point of view even if a suitable value of the magnetization parameter has been chosen.
Index Terms- Slider bearing; magnetic fluid; surface roughness; porosity; load carrying capacity.

1. INTRODUCTION:

Double layered porous plates are found to be useful in reducing the permeability in order to retain the lubricant between the plates and hence to improve performance when the porous plates are not completely saturated with lubricant. Marshall and Morgan [1] established that the use of double layered porous housing in which the inner layer has a reduced pore size and hence low permeability is advantageous because it reduces the seepage of the lubricant into the porous wall and helps to bring the lubricant between the surfaces during starvation period. Cusano [2] dealt with the lubrication of two layered porous journal bearing. Srinivasan [3] made use of the Morgan – Cameron approximation and simplified the analysis of two layered porous bearing. In fact, she considered the squeeze film behavior between two layered porous plates of various geometries and derived the expressions for various bearing performance characteristics in closed form. Gupta, Patel and Hingu [4] analyzed the problem of two layered porous journal bearing taking the curvature of the bearing into account. Bhat and Patel [5] discussed the problem of hydrodynamic lubrication of two layered porous slider bearing with tangential velocity slip. Besides, the following investigations (Circular plates of Patel and Hingu [6], annular plates studied by Hingu [7] and externally pressurized bearings by Ajawalia [8]) regarding the double layered bearings have been conducted. All the above investigations dealt with the conventional lubricants. Oil based or other lubricating fluid based magnetic fluid can act as a lubricant. The advantage of magnetic fluid as lubricant over the conventional ones is that the former can be retained at the desired location by an external magnetic field. Use of magnetic fluid as a lubricant improving the performance of the bearing system has now been very well recognized. Agrawal [9] considered the problem of slider bearing working with a magnetic fluid as the lubricant and found its performance better than the one with conventional lubricant. Bhat and Deheri [10] extended this analysis by considering a magnetic fluid based porous composite slider bearing with its slider consisting of an inclined pad and a flat pad. The effect of electric and magnetic fields on the flow of electrically conducting lubricants has been studied. Usually, two general configurations of the slider have been analyzed. One configuration uses a transverse magnetic field with tangential electric field while the other uses a tangential magnetic field with a tangential electric field. Bhat and Hingu [11] conducted a study of the hydromagnetic squeeze film between two layered porous rectangular plates. Here it was shown that MHD induces a relatively better performance.

But owing to elastic, thermal and uneven wear effects the configuration of the bearing encountered in practice are normally far from being smooth. It is an established fact that the bearing surfaces tend to be rough after receiving some run in and wear. Even sometimes the contaminations of lubricants and

chemical degradation of surfaces contribute to roughness. Tzeng and Seibel (1967) recognized the random character of the roughness of the bearing surfaces and used a stochastic approach to model the roughness mathematically. This approach of Tzeng and Seibel [12] was further developed and modified by Christensen and Tonder (1969.a, 1969.b, 1970) to study the effect of surface roughness in general. This analysis of Christensen and Tonder [13, 14, 15] was employed in several investigations (Ting [16] Prakash and Tiwari [17] Prajapati [18, 19], Guha [20], Gupta and Deheri [21] Andharia, Gupta and Deheri [22, 23]). Andharia, Gupta and Deheri [27] proved that the transverse surface roughness affected adversely on the hydrodynamic lubrication of slider bearings. However, it was noted that the negatively skewed roughness resulted in a relatively better situation. Lin et. al. [28] analyzed the surface roughness effect on the oscillating squeeze film behavior of a long partial journal bearing. According to the results found the effect of circumferential roughness provided a reduction in the mean bearing eccentricity ratio as compared to the smooth bearing case. However, the squeeze film bearing with longitudinal roughness structure resulted in a reverse trend. Patel and Deheri [29] discussed the effect of transverse surface roughness on the performance of a porous slider bearing with slip velocity under the presence of a magnetic fluid lubricant. It was shown that the negatively skewed roughness increase the load carrying capacity which was already increased by the magnetization. It was established that for an overall improved performance the slip velocity deserve to be kept at minimum. Recently, Patel, Deheri and Vadher [24] considered the effect of transverse surface roughness on magnetic fluid based squeeze film performance between porous infinitely long parallel plates with porous matrix of non-uniform thickness. Patel and Deheri [30] discussed the magnetic squeeze film performance in a double layered rough porous slider bearing taking combined porous structures. Recently, Patel and Deheri [31]dealt with the comparison of different porous structures on the performance of a magnetic fluid based porous layered rough slider bearing.

Here it has been proposed to study the effect of transverse surface roughness on the performance of a magnetic fluid based porous two layered inclined slider bearing.

2. ANALYSIS:

The configuration of the bearing which is infinite in the Z – direction is shown below.

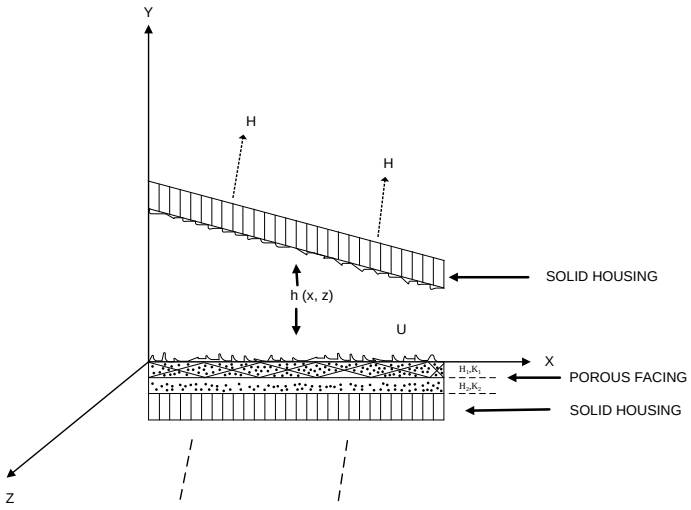

Configuration of the bearing system

The non-porous slider moves with a uniform velocity U in the X – direction. The stator has porous facing of thickness H1 and H2 backed by solid housing. The applied magnetic field $\bar{H}$ is oblique to the stator. The governing differential equations for the motion of magnetic fluid, continuity equation and Maxwell equations in the film region are (Agrawal (1986))

$$\rho\left[\frac{\partial\vec{V}}{\partial t}+(\vec{V}.\nabla)\vec{V}\right]=-\nabla p+\mu\nabla^2\vec{V}+\mu_0(\vec{M}.\nabla)\vec{H}+\rho\alpha^2\nabla\times\left(\frac{\vec{M}}{M}+M^*\right) \quad (1)$$

$$\nabla.\vec{V}=0 \quad (2)$$

$$\nabla\times\vec{H}=0 \quad (3)$$

$$\nabla.\vec{B}=0,\ \vec{B}=\mu_0(\vec{H}+\vec{M}) \quad (4)$$

and

$$\vec{M}=\bar{\mu}\ \vec{H}$$

where $\vec{V}$, π, ρ, μ, α, , M, M∗, $\vec{H}$, $\bar{\mu}$ and μ0 are the fluid velocity, the lubricant pressure, the density, the coefficient of viscosity, a material constant, the magnetization vector, the magnitude of the magnetization vector, the corotational derivative of , the external magnetic field, the magnetic susceptibility and the free space permeability respectively. With usual assumptions of lubrication and neglecting the self-field created by the magnetization of the fluid, Equations (1) and (2) reduce to

$$-\frac{\partial p}{\partial x}+\mu\frac{\partial^2 u}{\partial y^2}+\mu_0\left(M_1\frac{\partial H_x}{\partial x}+M_2\frac{\partial H_x}{\partial y}\right)=0 \quad (6)$$

$$-\frac{\partial p}{\partial x}+\mu_0\left(M_1\frac{\partial H_y}{\partial x}+M_2\frac{\partial H_y}{\partial y}\right)=0 \quad (7)$$

and

$$\frac{\partial u}{\partial x}+\frac{\partial u}{\partial y}=0 \tag{8}$$

where (M1, M2) and (Hx, Hy) are the components of the magnetization and the external field , which is applied obliquely.

The flow of the magnetic fluid in the porous regions are given by:

(Region: - H1 < y < 0)

$$\overrightarrow{u_1}=-\left(\frac{K_1}{\mu}\right)\frac{\partial\overrightarrow{p_1}}{\partial x}+\left(\frac{\mu_0 K_1}{\mu}\right)\left(M_1\frac{\partial H_x}{\partial x}+M_2\frac{\partial H_x}{\partial y}\right) \tag{9}$$

$$\overrightarrow{v_1}=-\left(\frac{K_1}{\mu}\right)\frac{\partial\overrightarrow{p_1}}{\partial y}+\left(\frac{\mu_0 K_1}{\mu}\right)\left(M_1\frac{\partial H_y}{\partial x}+M_2\frac{\partial H_y}{\partial y}\right) \tag{10}$$

and

$$\frac{\partial\overrightarrow{u_1}}{\partial x}+\frac{\partial\overrightarrow{v_1}}{\partial y}=0 \tag{11}$$

(Region: - $(H_1 + H_2) \le y < - H_1$)

$$\overrightarrow{u_2}=-\left(\frac{K_2}{\mu}\right)\frac{\partial\overrightarrow{p_2}}{\partial x}+\left(\frac{\mu_0 K_2}{\mu}\right)\left(M_1\frac{\partial H_x}{\partial x}+M_2\frac{\partial H_x}{\partial y}\right) \tag{12}$$

$$\overrightarrow{v_2}=-\left(\frac{K_2}{\mu}\right)\frac{\partial\overrightarrow{p_2}}{\partial y}+\left(\frac{\mu_0 K_2}{\mu}\right)\left(M_1\frac{\partial H_y}{\partial x}+M_2\frac{\partial H_y}{\partial y}\right) \tag{13}$$

And

$$\frac{\partial\overrightarrow{u_2}}{\partial x}+\frac{\partial\overrightarrow{v_2}}{\partial y}=0 \tag{14}$$

where K_1 and K_2 are the permeabilities and H_1 and H_2 are the thickness of the porous bushes, $\overrightarrow{p_1}$ and $\overrightarrow{p_2}$ are the pressure in the respective two porous regions.

From Equations (3) and (5)

$$H_x=-\frac{\partial\phi}{\partial x},\ H_y=-\frac{\partial\phi}{\partial y} \tag{15}$$

and

$M_1 = \bar{\mu}H_x$, $M_2 = \bar{\mu}H_y$, $H^2 = H_x^2 + H_y^2$ (16)

Also,

$$M_1\frac{\partial H_x}{\partial x}+M_2\frac{\partial H_x}{\partial y}=\bar{\mu}\left(\frac{\partial\phi}{\partial x}\cdot\frac{\partial^2\phi}{\partial x^2}+\frac{\partial\phi}{\partial y}\cdot\frac{\partial^2\phi}{\partial x\partial y}\right)$$

$$=\frac{\bar{\mu}}{2}\frac{\partial}{\partial x}H^2 \tag{17}$$

and

$$M_1\frac{\partial H_y}{\partial x}+M_2\frac{\partial H_y}{\partial y}=\bar{\mu}\left(\frac{\partial\phi}{\partial x}\cdot\frac{\partial^2\phi}{\partial x\partial y}+\frac{\partial\phi}{\partial y}\cdot\frac{\partial^2\phi}{\partial y^2}\right)$$

$$=\frac{\bar{\mu}}{2}\frac{\partial}{\partial y}H^2 \tag{18}$$

Substitution of Equation (17) into Equation (6); Equation (18) into Equation (7) respectively, gives

$$\mu\frac{\partial^2 u}{\partial y^2}-\frac{\partial}{\partial x}\left(p-\frac{\mu_0\bar{\mu}H^2}{2}\right)=0 \tag{19}$$

$$-\frac{\partial}{\partial y}\left(p-\frac{\mu_0\bar{\mu}H^2}{2}\right)=0 \tag{20}$$

Similarly, the Equations (9), (10), (12) and (13) turn to

$$\overrightarrow{u_1}=-\left(\frac{K_1}{\mu}\right)\frac{\partial}{\partial x}\left(\overrightarrow{p_1}-\frac{\mu_0\bar{\mu}H^2}{2}\right) \tag{21}$$

$$\overrightarrow{v_1}=-\left(\frac{K_1}{\mu}\right)\frac{\partial}{\partial y}\left(\overrightarrow{p_1}-\frac{\mu_0\bar{\mu}H^2}{2}\right) \tag{22}$$

$$\overrightarrow{u_2}=-\left(\frac{K_2}{\mu}\right)\frac{\partial}{\partial x}\left(\overrightarrow{p_2}-\frac{\mu_0\bar{\mu}H^2}{2}\right) \tag{23}$$

$$\overrightarrow{v_2}=-\left(\frac{K_2}{\mu}\right)\frac{\partial}{\partial y}\left(\overrightarrow{p_2}-\frac{\mu_0\bar{\mu}H^2}{2}\right) \tag{24}$$

Substituting from Equations (21) and (22) into Equation (11) one avails

$$\frac{\partial^2}{\partial x^2}\left(\overrightarrow{p_1}-\frac{\mu_0\bar{\mu}H^2}{2}\right)+\frac{\partial^2}{\partial y^2}\left(\overrightarrow{p_1}-\frac{\mu_0\bar{\mu}H^2}{2}\right)=0 \tag{25}$$

and substituting Equations (23) and (24) into Equations (14) one obtains:

$$\frac{\partial^2}{\partial x^2}\left(\overline{p_2}-\frac{\mu_0\bar{\mu}\bar{H}^2}{2}\right)+\frac{\partial^2}{\partial y^2}\left(\overline{p_2}-\frac{\mu_0\bar{\mu}\bar{H}^2}{2}\right)=0 \tag{26}$$

Now solving Equation (19) using boundary conditions

u = 0 at y = 0

and

u = U at y = h,

one can conclude that

$$u=\frac{1}{2\mu}\frac{\partial}{\partial x}\left(p-\frac{\mu_0\bar{\mu}\bar{H}^2}{2}\right)(y^2-hy)+\frac{Uy}{h} \tag{27}$$

Substitution of Equation (27) into Equation (8) and integration across the film thickness gives

$$(v)_{y=0}=\frac{\partial}{\partial x}\left[-\frac{h^3}{12\mu}\frac{\partial}{\partial x}\left(p-\frac{\mu_0\bar{\mu}\bar{H}^2}{2}\right)+\frac{Uh}{2}\right] \tag{28}$$

Since the velocity component in the y – direction must be continuous at the plate–film interface.

$$(v)_{y=0}=\left(\overline{v_1}\right)_{y=0} \tag{29}$$

while the other boundary conditions are

while the other boundary conditions are

$\bar{p} = \bar{p}_1$ at y = 0 (30)

$\bar{v}_2 = \bar{v}_1$ at y = - H_1 (31)

$\bar{p}_2 = \bar{p}_1$ at y = - H_1 (32)

$\bar{v}_2 = 0$ at y = - (H_1+H_2) (33)

From Equation (33) with Taylor's series expansion one obtains

$$\left(\overline{v_2}\right)_{-(H_1+H_2)}=\left(\overline{v_2}\right)_{-H_1}-H_2\left(\frac{\partial\overline{v_2}}{\partial y}\right)_{-H_1}+\ldots=0$$

Neglecting higher powers of H_1, assuming it small

$$\left(\overline{v_2}\right)_{-H_1}=-H_2\left(\frac{\partial\overline{v_2}}{\partial y}\right)_{-H_1}$$

Using Equation (31)

$$\left(\overline{v_1}\right)_{-H_1}=-H_2\left(\frac{\partial\overline{v_1}}{\partial y}\right)_{-H_1}$$

Expanding left hand side by Maclaurin's series and using Equation (24) it is found that

$$\left(\overline{v_1}\right)_{y=0}-H_1\left(\frac{\partial\overline{v_1}}{\partial y}\right)_{y=0}=H_2\frac{\partial}{\partial y}\left[-\frac{K_2}{\mu}\frac{\partial}{\partial y}\left(\overline{p_1}-\frac{\mu_0\bar{\mu}\bar{H}^2}{2}\right)\right]_{y=-H_1}$$

$$=\left[-\frac{K_2H_2}{\mu}\frac{\partial^2}{\partial y^2}\left(\overline{p_1}-\frac{\mu_0\bar{\mu}\bar{H}^2}{2}\right)\right]_{y=-H_1}$$

Using Equation (32) and further expanding it by Maclaurin's series one arrives at

$$\left(\overline{v_1}\right)_{y=0}=H_1\left(\frac{\partial\overline{v_1}}{\partial y}\right)_{y=0}$$

$$\left[-\frac{K_2H_2}{\mu}\frac{\partial^2}{\partial y^2}\left(\overline{p_1}-\frac{\mu_0\bar{\mu}\bar{H}^2}{2}\right)\right]_{y=0}$$

$$+O(H_2)$$

In view of Equation (22) this leads to

$$\left(\overline{v_1}\right)_{y=0}=-\left[\frac{K_1H_1}{\mu}\frac{\partial^2}{\partial y^2}\left(\overline{p_1}-\frac{\mu_0\bar{\mu}\bar{H}^2}{2}\right)\right]_{y=0}$$

$$-\left[\frac{K_2H_2}{\mu}\frac{\partial^2}{\partial y^2}\left(\overline{p_1}-\frac{\mu_0\bar{\mu}\bar{H}^2}{2}\right)\right]_{y=0}$$

$$\left(\overline{v_1}\right)_{y=0}=-\left[\frac{\left(K_1H_1+K_2H_2\right)}{\mu}\frac{\partial^2}{\partial x^2}\left(p-\frac{\mu_0\bar{\mu}\bar{H}^2}{2}\right)\right] \tag{34}$$

by making use of use of Equation (30). Use of Equation (34) in Equation (28) gives

$$\frac{\partial}{\partial x}\left[\left\{\left(\frac{K_1H_1+K_2H_2}{\mu}\right)+\frac{h^3}{12\mu}\right\}\frac{\partial}{\partial x}\left(p-\frac{\mu_0\bar{\mu}\bar{H}^2}{2}\right)\right]=\frac{U}{2}\frac{dh}{dx} \tag{35}$$

Integrating Equation (35) one observes that

$$\frac{\partial}{\partial x}\left(p-\frac{\mu_0\bar{\mu}\bar{H}^2}{2}\right)=\frac{\mu(6Uh-12A)}{h^3+12\left(K_1H_1+K_2H_2\right)} \quad (36)$$

where A is a constant of integration.

In view of the discussions ensued in Christensen and Tonder [13 14 15] regarding the stochastic modeling of roughness, the thickness h(x) of the lubricant film is considered as

$h(x) = \bar{h}(x) + h_s(x)$

where $\bar{h}(x)$ is the mean film thickness and $h_s(x)$ is the deviation from the mean film thickness characterizing the random roughness of the bearing surfaces. $H_s(x)$ is considered to be stochastic in nature and governed by the probability density function f (h_s), $-c \le h_s \le c$ where c is the maximum deviation from the mean film thickness. The meanα, the standard deviation σ and the parameter ε which is the measure of symmetry of random variable h_s, are defined by relationships

$\alpha = E(h_s)$

$\sigma^2 = E[(h_s - \alpha)^2]$

and

$\varepsilon = E[(h_s - \alpha)^3]$

where the expectancy operator E is defined by

$$E\,I = \int_{-c}^{c} R f(h_s)\,dh_s$$

while

$$f(h_s)=\begin{cases}\dfrac{35}{32c^7}(c^2-h_s^2)^3, & \text{if } -c<h_s<c\\ 0, & \text{elsewhere}\end{cases}$$

Owing to the fact that the self-field created by the magnetization is ignored, Equation (4) is identically satisfied. Following Agrawal [9] magnitude of applied magnetic field H should be a function of x. It is assumed that the applied magnetic field has components of the form,

$H_x = H(x)\cos[\theta(x, y)]$, $H_y = H(x)\sin[\theta(x, y)]$ and $H_z = 0$

H^2 should satisfy the condition that it becomes zero at the interface of the bearing and the atmosphere that is $H^2(x) = 0$ at x = 0 and L. Hence, $\nabla \times \vec{H} = 0$ in the present case becomes

$$\frac{\partial H_y}{\partial x}-\frac{\partial H_x}{\partial y}=0$$

Thus, one gets the equation for the inclination of the magnetic field $\theta(x, y)$ as

$$\cot\theta\frac{\partial\theta}{\partial x}+\frac{\partial\theta}{\partial y}=-\frac{1}{H}\frac{\partial H}{\partial x}$$

With the suitable choice of H(x) the solution of this partial differential equation gives the inclination θ.

Following Prajapati (1995), here it is considered that

$H^2 = x(L - x)$,

where L is the length of the bearing along x – axis. Hence,

$$\cot\theta\frac{\partial\theta}{\partial x}+\frac{\partial\theta}{\partial y}=-\frac{(L-2x)}{2x(L-x)}$$

whose solution is C eliminant of

$\operatorname{cosec}^2\theta = C^2(Lx - x^2)$

and

$C(2x - L) = \{C^2L^2 - 4\sin(Cy)\}^{1/2}$

When the dimensionless quantities are introduced as follows

$$\bar{x}=\frac{x}{L} \qquad \bar{h}=\frac{h}{h_0} \qquad p^*=\frac{ph_0^2}{\mu UL}$$

$$\mu^*=\frac{\mu_0\bar{\mu}\bar{h}_0^2L}{\mu U} \qquad \bar{A}=\frac{12A}{Uh_0}$$

$$\beta^3=\frac{12\left(K_1H_1+K_2H_2\right)}{h_0^3}=12\left(\psi_1+\psi_2\right)$$

$$\psi_1=\frac{K_1H_1}{h_0^3} \qquad \psi_2=\frac{K_2H_2}{h_0^3}$$

$$\sigma^*=\frac{\sigma}{h_0} \qquad \alpha^*=\frac{\alpha}{h_0} \qquad \varepsilon^*=\frac{\varepsilon}{h_0^3},$$

Equation (36) becomes

$$\frac{\partial}{\partial\bar{x}}\left(p^*-\frac{\mu^*}{2}\bar{x}(1-\bar{x})\right)=\frac{6\bar{h}-\bar{A}}{g(\bar{h})} \quad (37)$$

where

$$g(\bar{h})=\bar{h}^3+3\sigma^{*2}\bar{h}+3\bar{h}^2\alpha^*+3\bar{h}\alpha^{*2}+3\sigma^{*2}\alpha^*+\alpha^{*3}+\varepsilon^*+12\beta^3$$

In non-dimensional form the thickness of the fluid film is given by

$$\bar{h} = a - (a - 1)\,\bar{x} \quad (38)$$

where $a = h_1 / h_0$, h_0 and h_1 are values of h at x = 0 and x = L. Integrating Equation (37) with boundary conditions,

$p^* = 0$ at $\bar{x} = 0$ (39)

$p^* = 0$ at $\bar{x} = 1$ (40)

one gets the pressure distribution in dimensionless form as

$$p^*=\frac{\mu^*}{2}\bar{x}(1-\bar{x})+\int_0^{\bar{x}}\left(\frac{6\bar{h}-\bar{A}}{g(\bar{h})}\right)d\bar{x} \quad (41)$$

where

$$\bar{A} = \frac{\int_0^1 \left(\frac{6\bar{h}\, d\bar{x}}{g(\bar{h})} \right)}{\int_0^1 \left(\frac{d\bar{x}}{g(\bar{h})} \right)} \qquad (42)$$

The load carrying capacity is obtained from

$$W = B \int_0^L p\, dx$$

which in non-dimensional form becomes

$$\bar{W} = \frac{W h_0^2}{\mu B U L^2} = \int_0^1 p^* d\bar{x}$$

$$= \frac{\mu^*}{12} + \int_0^1 \left(\frac{(\bar{A} - 6\bar{h})\bar{x}}{g(\bar{h})} \right) d\bar{x} \qquad (43)$$

where B is the Z – width of the bearing.

The position of the centre of pressure is

$$\bar{x} = \frac{x}{L} = \frac{1}{2\bar{W}} \left[- \int_0^1 \left(\frac{(\bar{A} - 6\bar{h})\bar{x}^2}{g(\bar{h})} d\bar{x} \right) + \frac{\mu^*}{12} \right] \qquad (44)$$

The frictional force is

$$F = \mu B \int_0^L \left(\frac{\partial u}{\partial y} \right)_{y=h} dx$$

which in dimensionless form turns to

$$\bar{F} = \frac{h_0 F}{\mu B L U} = \int_0^1 \left[\frac{\bar{h}}{2} \frac{\partial}{\partial \bar{x}} \left(p^* - \frac{\mu^*}{2} \bar{x}(1 - \bar{x}) \right) + \frac{1}{\bar{h}} \right] d\bar{x} \qquad (45)$$

Lastly, the dimensionless coefficient of friction is calculated from

$$\bar{f} = \frac{\bar{F}}{\bar{W}} \qquad (46)$$

where $\bar{F}$ and $\bar{W}$ are given by Equations (45) and (43) respectively.

3. RESULTS AND DISCUSSION:

It is clearly seen that the non-dimensional pressure distribution is obtained from Equation (41) while Equation (43) determines dimensionless load carrying capacity. Besides, the non-dimensional friction can be obtained from equation (45) while equation (44) determines the position of centre of pressure. It may be easily observed that the use of magnetic fluid as a lubricant in place of conventional non-magnetic lubricant results in the increase of lubricant pressure by $\frac{\mu^* \bar{X}(1 - \bar{X})}{2}$ and the increase of load carrying capacity by $\frac{\mu^*}{12}$. It is noticed that the coefficient of friction $\bar{f}$ decreases while the shearing friction $\bar{F}$ remains almost unaffected.

The extent of change in the performance characteristics suggests that the bearing performance tends to become superior in spite of the fact that the bearing suffers owing to transverse surface roughness. However, interestingly it may be noted that the extent of change in bearing performance characteristic due to the use of magnetic fluid lubricant is irrespective of the fact that whether the bearing is single layered or multi layered porous or even non-porous. Setting the magnetization parameter to be zero for a bearing with smooth surfaces this investigation reduces to the study of Srinivasan [3].

The variation of non-dimensional load carrying capacity with respect to the thickness ratio presented in Figures (1 – 5) makes it clear that the load carrying capacity increases sharply with the increase in the thickness ratio. However, the effect of standard deviation and skewness with respect thickness ratio is almost negligible, while, the effect of magnetic fluid lubricant is negligible up to 0.01. Figures (6 – 9) dealing with the effect of magnetic fluid lubricant indicate that the load carrying capacity sharply increases with increasing values of magnetization. However, the effect of standard deviation and skewness on the distribution of load carrying capacity with respect to magnetization is almost negligible.

The effect of the porosity parameter depicted in Figures (10 – 12) makes it clear that the porosity induces sharp decrease in the load carrying capacity. However, here also, the effect of standard deviation and skewness on the load carrying capacity with respect to porosity is almost negligible. The fact that standard deviation reduces the load carrying capacity substantially is manifest in Figures (13 – 14). Further, it is seen from Figures (13 – 15) that the negatively skewed roughness increases the load carrying capacity while the load decreases due to positively skewed roughness. Similarly the load carrying capacity decreases due to positive variance, while, the load carrying capacity increases considerably because of variance (–ve).

Mostly, the friction decreases as can be seen from Figures (16 – 30). There is minor increase in the friction due to the transverse surface roughness but the porosity induces some increase in the friction which is unlike the findings of the discussion of Prajapati [25]. A close glance at the Tables (1 – 15) reveals that the position of centre of pressure remains almost unaffected by the magnetization, however, it negligibly shifts towards the bearing's outlet.

The expression for $\beta^3 = 12(\psi_1 + \psi_2)$ conveys that an additional porous layer gives an additional degree of freedom for a proper bearing design. Some of the figures tend to suggest that parameters ψ_1 and ψ_2 may be chosen in such a way that while β^3 remains at minimum for better performance of the bearing, relatively better physical advantages for copious supply of lubricant from the porous matrix into the film space may be available during starvation period.

From Figures (3), (5), (7), (9), (10) and (12) one can easily notice that the roughness parameters namely, standard deviation and skewness fail to produce a significant effect unlike the case of earlier studies. (Prajapati [25], Deheri et. Al [26]). A key point to be noted is that for an improved performance of the bearing system the variance plays a seminal role which is a study in contrast as the negatively skewed roughness plays a central role in this improvement as found in (Deheri et. Al [26])

4. CONCLUSION

This study makes it mandatory that the roughness must be given due consideration while designing the bearing system. This article not only offers an additional degree of freedom from design point of view but also establishes that the bearing can support a load even when there is the absence of flow. This investigation offers some measures to compensate the adverse effect of roughness and porosity by the positive effect of magnetic fluid lubricant especially when variance (–ve) occurs. This evaluation is all the more necessary from bearings life period point of view. In addition, it is revealed that this type of bearing system can support a load even in the absence of flow, unlike the case of a conventional lubricant.

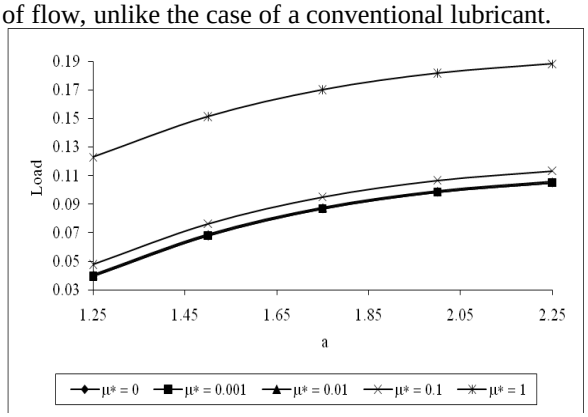

Figure: 1 Variation of load carrying capacity with respect to a and μ*

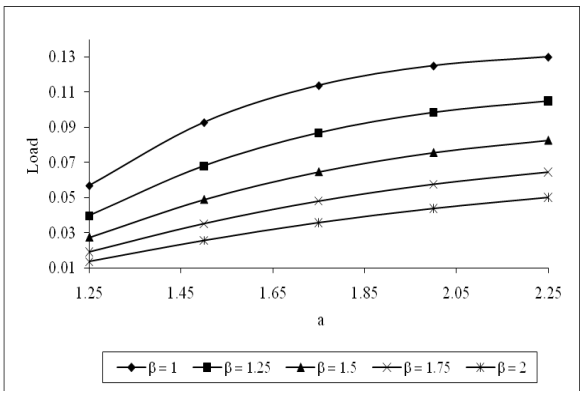

Figure: 2 Variation of load carrying capacity with respect to a and β

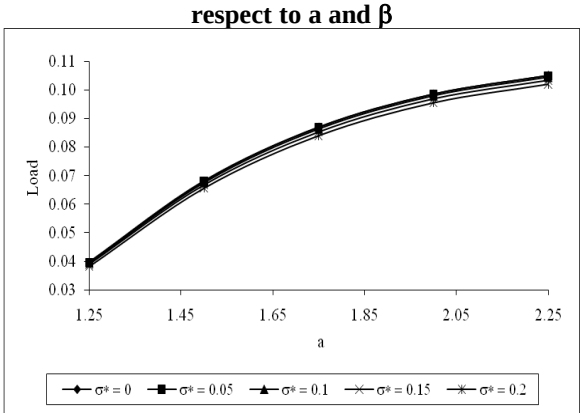

Figure: 3 Variation of load carrying capacity with respect to a and σ*

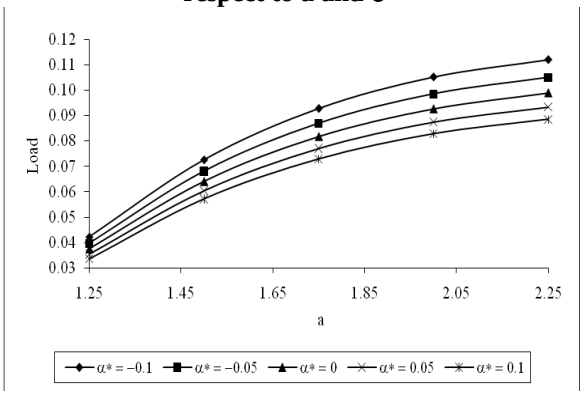

Figure: 4 Variation of load carrying capacity with respect to a and α*

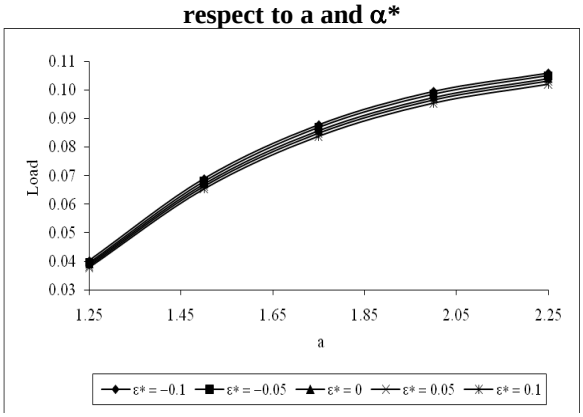

Figure: 5 Variation of load carrying capacity with respect to a and ε*

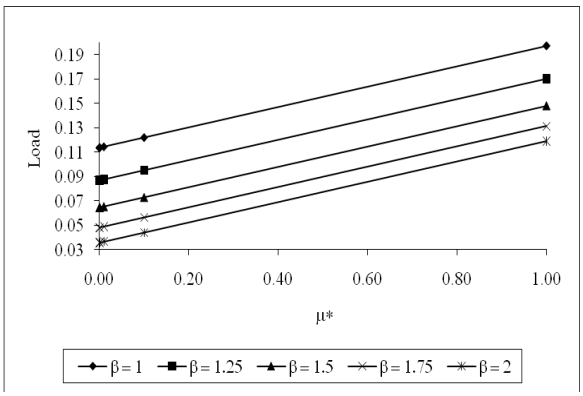

Figure: 6 Variation of load carrying capacity with respect to μ* and β

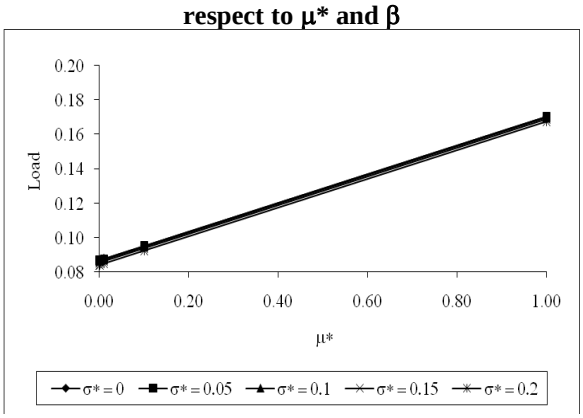

Figure: 7 Variation of load carrying capacity with respect to μ* and σ*

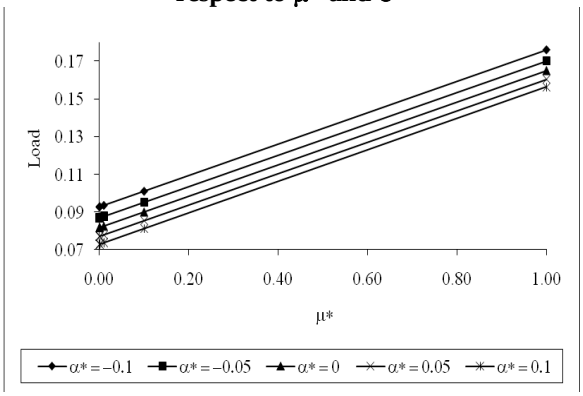

Figure: 8 Variation of load carrying capacity with respect to μ* and α*

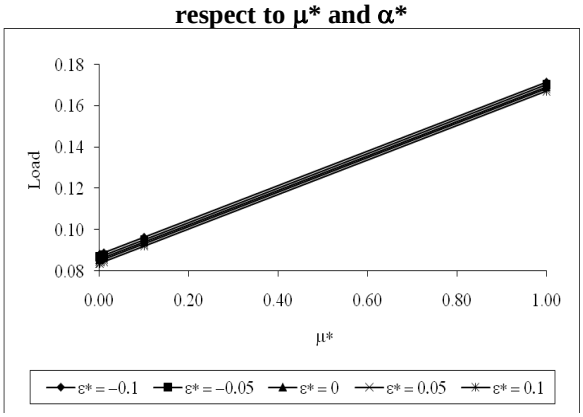

Figure: 9 Variation of load carrying capacity with respect to μ* and ε*

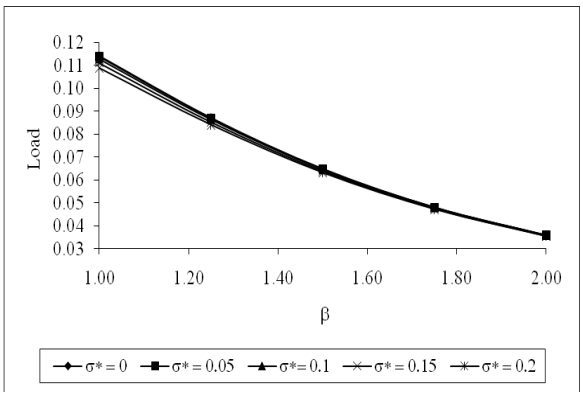

Figure: 10 Variation of load carrying capacity with respect to β and σ*

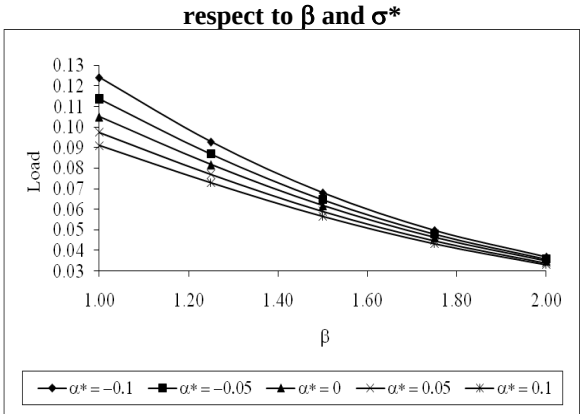

Figure: 11 Variation of load carrying capacity with respect to β and α*

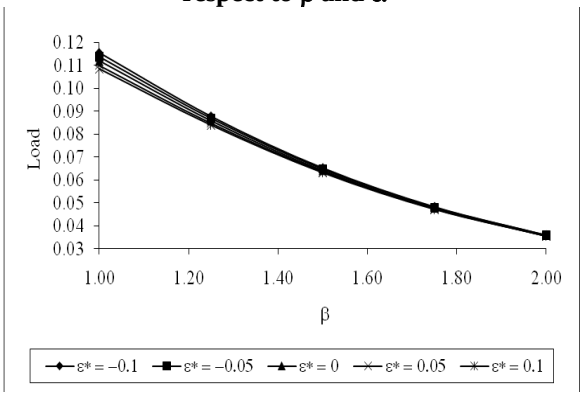

Figure: 12 Variation of load carrying capacity with respect to β and ε*

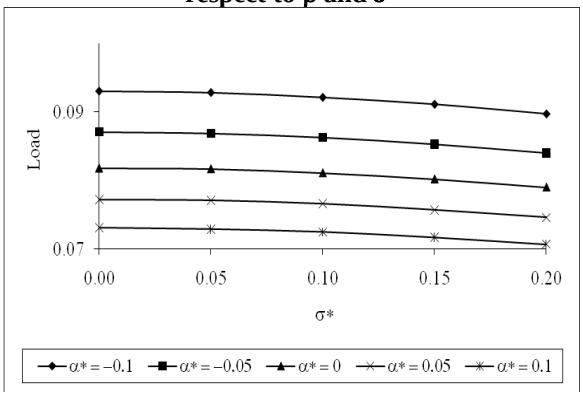

Figure: 13 Variation of load carrying capacity with respect to σ* and α*

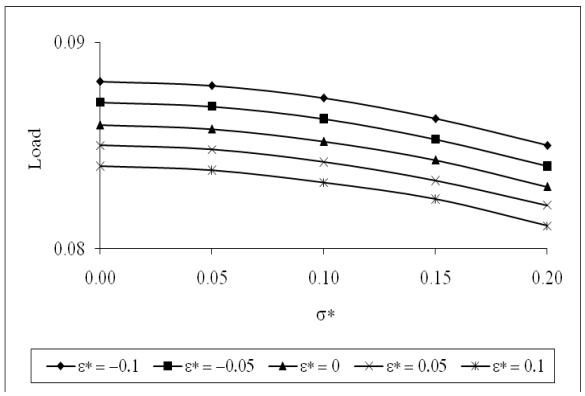

Figure: 14 Variation of load carrying capacity with respect to σ* and ε*

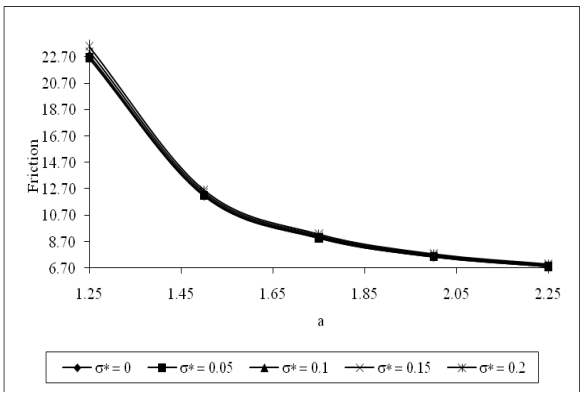

Figure: 18 Variation of frictional force with respect to a and σ*

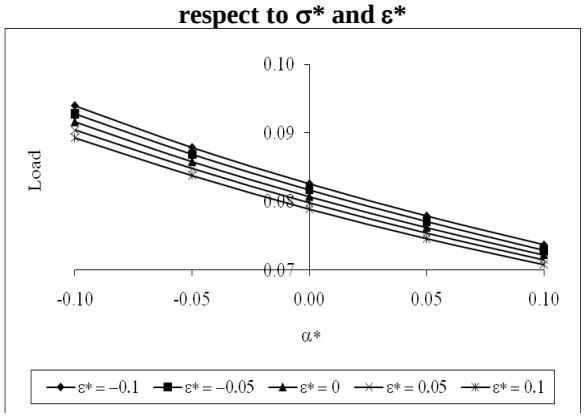

Figure: 15 Variation of load carrying capacity with respect to α* and ε*

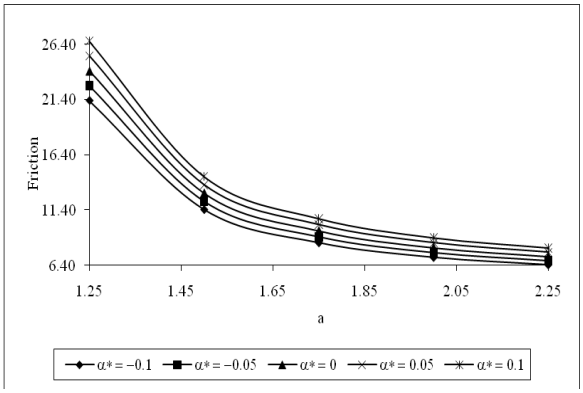

Figure: 19 Variation of frictional force with respect to a and α*

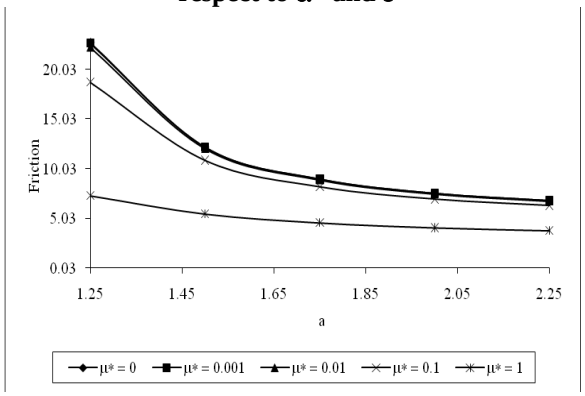

Figure: 16 Variation of frictional force with respect to a and μ*

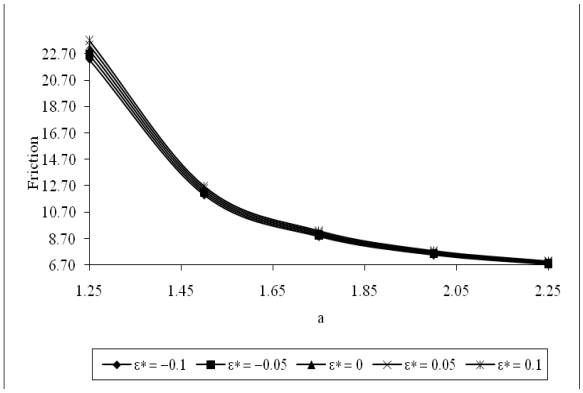

Figure: 20 Variation of frictional force with respect to a and ε*

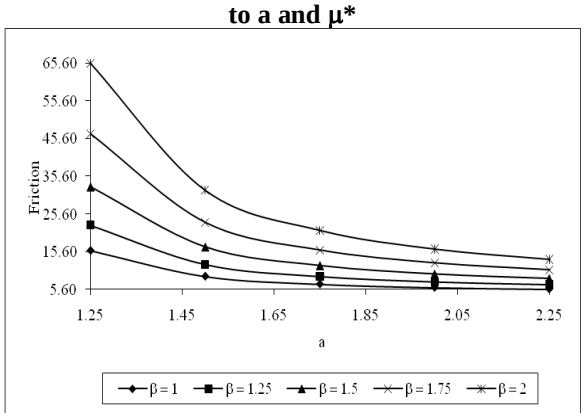

Figure: 17 Variation of frictional force with respect to a and β

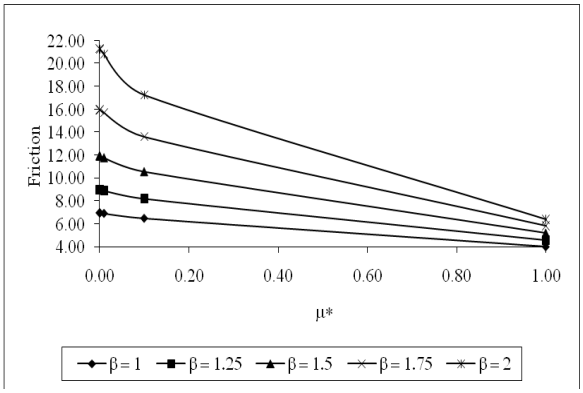

Figure: 21 Variation of frictional force with respect to μ* and β

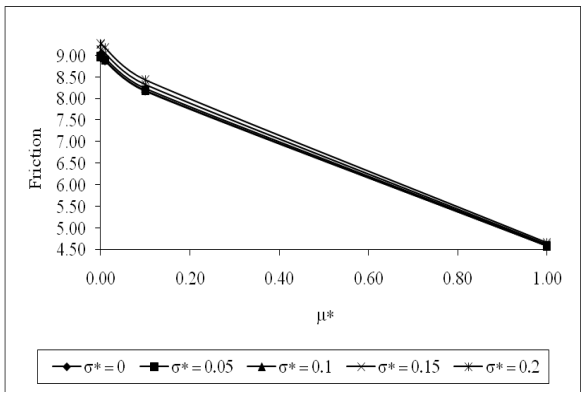

Figure: 22 Variation of frictional force with respect to μ* and σ*

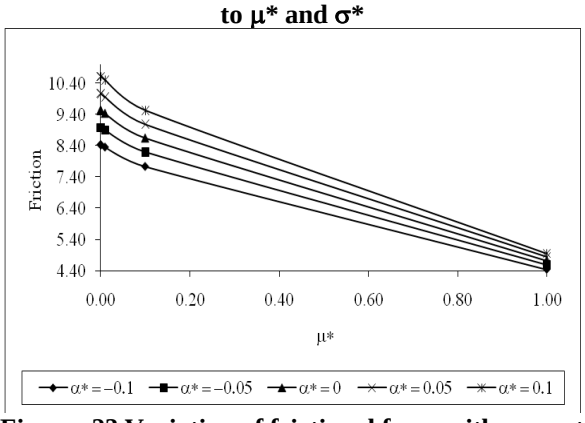

Figure: 23 Variation of frictional force with respect to μ* and α*

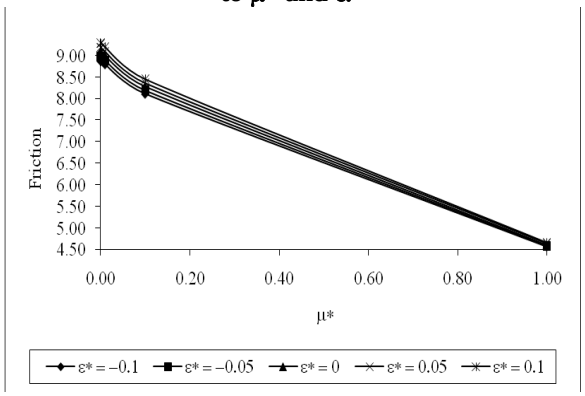

Figure: 24 Variation of frictional force with respect to μ* and ε*

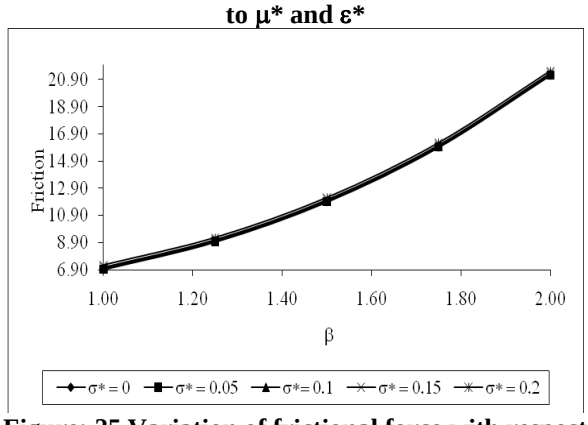

Figure: 25 Variation of frictional force with respect to β and σ*

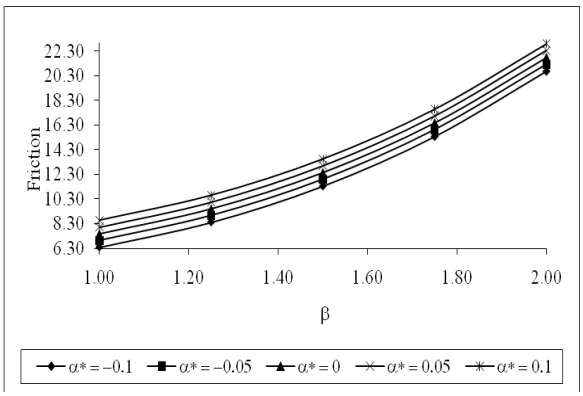

Figure: 26 Variation of frictional force with respect to β and α*

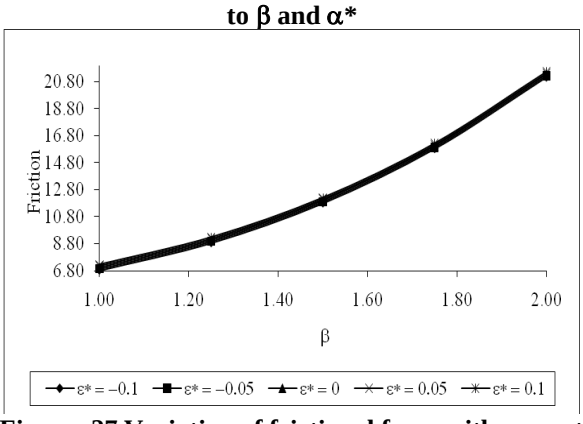

Figure: 27 Variation of frictional force with respect to β and ε*

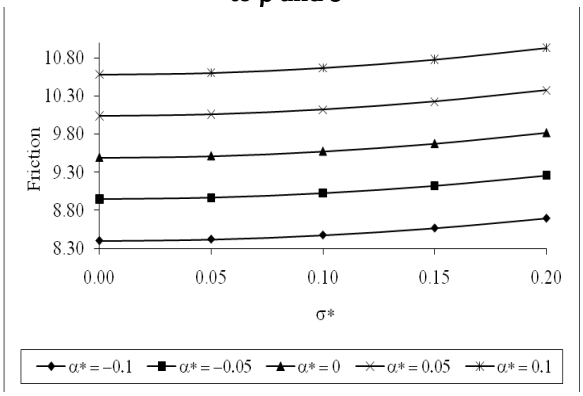

Figure: 28 Variation of frictional force with respect to σ* and α*

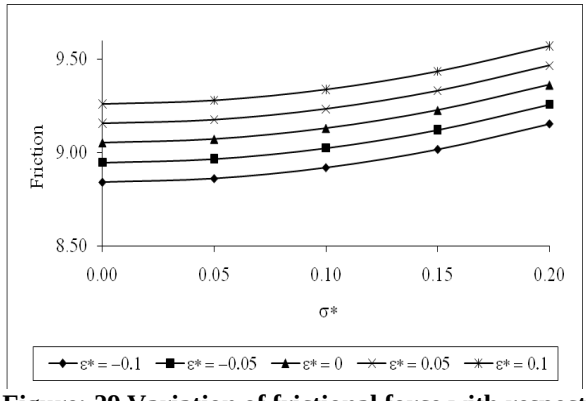

Figure: 29 Variation of frictional force with respect to σ* and ε*

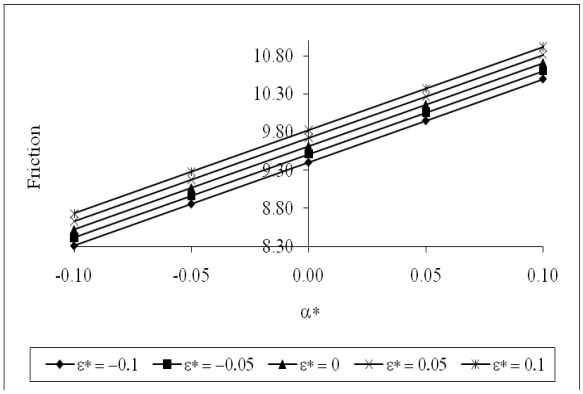

Figure: 30 Variation of frictional force with respect to α* and ε*

Table : 1 Variation of centre of pressure with respect to μ* and a					
σ*= 0.05, α* = –0.05 , ε* = –0.05 , β = 1.25					
	a = 1.25	a = 1.5	a = 1.75	a = 2	a = 2.25
μ* = 0	1.213700	1.771900	61.995400	31.025800	18.849500
μ* = 0.001	1.211200	1.769700	61.936400	31.000000	18.835000
μ* = 0.01	1.188700	1.750400	61.410500	30.769500	18.704900
μ* = 0.1	1.002600	1.578800	56.607000	28.642700	17.499400
μ* = 1	391.070000	79.843300	31.869000	17.029000	10.727200
Table : 2 Variation of centre of pressure with respect to β and a					
σ*= 0.05, α* = –0.05 , ε* = –0.05 , μ* = 0.001					
	a = 1.25	a = 1.5	a = 1.75	a = 2	a = 2.25
β = 1	8.438300	1.298900	47.425300	24.554900	15.331900
β = 1.25	1.211200	1.769700	61.936400	31.000000	18.835000
β = 1.5	1.756200	2.461400	82.946300	40.179400	23.744300
β = 1.75	2.513800	3.418100	1.117300	52.602700	30.300900
β = 2	3.518100	468.422200	1.496100	68.821000	38.777000
Table : 3 Variation of centre of pressure with respect to σ* and a					
β= 1.25, α* = –0.05 , ε* = –0.05 , μ* = 0.001					
	a = 1.25	a = 1.5	a = 1.75	a = 2	a = 2.25
σ* = 0	1.208100	1.765400	61.797400	30.935800	18.799200
σ* = 0.05	1.211200	1.769700	61.936400	31.000000	18.835000
σ* = 0.1	1.220400	178.249000	62.353400	31.192300	18.942200
σ* = 0.15	1.235700	1.803800	63.048400	31.512800	19.121000
σ* = 0.2	1.257200	1.833700	64.021100	31.961300	19.371000
Table : 4 Variation of centre of pressure with respect to α* and a					
β= 1.25, σ* = 0.05 , ε* = –0.05 , μ* = 0.001					
	a = 1.25	a = 1.5	a = 1.75	a = 2	a = 2.25
α* = –0.1	1.138300	1.658500	58.018800	29.070700	17.698100
α* = –0.05	1.211200	1.769700	61.936400	31.000000	18.835000
α* = 0	1.283600	1.880400	65.840700	32.923500	19.968700
α* = 0.05	1.356100	1.991100	69.743200	34.846200	21.102000
α* = 0.1	1.428800	2.102000	73.655400	36.773300	22.237600

Table : 5 Variation of centre of pressure with respect to ε∗ and a

β= 1.25, σ∗ = 0.05 , α∗ = –0.05 , μ∗ = 0.001

	a = 1.25	a = 1.5	a = 1.75	a = 2	a = 2.25
ε∗ = –0.1	1.191900	174.519100	61.186900	30.669700	18.656800
ε∗ = –0.05	1.211200	1.769700	61.936400	31.000000	18.835000
ε∗ = 0	1.230400	1.794200	62.685000	31.329500	19.012600
ε∗ = 0.05	1.249600	1.818600	63.432600	31.658500	19.189800
ε∗ = 0.1	1.268800	1.843100	64.179300	31.986800	19.366500

Table : 6 Variation of centre of pressure with respect to μ* and β

σ∗= 0.05, α∗ = – 0.05, ε∗ = – 0.05, a = 1.75

	β = 1	β = 1.25	β = 1.5	β = 1.75	β = 2
μ∗ = 0	47.459700	61.995400	83.052600	111.923400	1.499600
μ∗ = 0.001	47.425300	61.936400	82.946300	111.729800	1.496100
μ∗ = 0.01	47.117900	61.410500	82.001600	110.017000	1.465500
μ∗ = 0.1	44.252100	56.607000	73.623200	95.403300	1.216700
μ∗ = 1	27.595300	31.869000	36.556600	41.154700	45.314100

Table : 7 Variation of centre of pressure with respect to μ* and σ∗

β= 1.25, α∗ = – 0.05, ε∗ = – 0.05, a = 1.75

	σ∗ = 0	σ∗ = 0.05	σ∗ = 0.1	σ∗ = 0.15	σ∗ = 0.2
μ∗ = 0	61.856100	61.995400	62.413300	63.109500	64.084100
μ∗ = 0.001	61.797400	61.936400	62.353400	63.048400	64.021100
μ∗ = 0.01	61.273800	61.410500	61.820300	62.503300	63.458900
μ∗ = 0.1	56.491000	56.607000	56.954500	57.532800	58.340400
μ∗ = 1	31.832700	31.869000	31.977200	32.156100	32.403200

Table : 8 Variation of centre of pressure with respect to μ* and α∗

σ∗= 0.05, β = 1.25, ε∗ = – 0.05, a = 1.75

	α∗ = –0.1	α∗ = –0.05	α∗ = 0	α∗ = 0.05	α∗ = 0.1
μ∗ = 0	58.070500	61.995400	65.907500	69.818200	73.739100
μ∗ = 0.001	58.018800	61.936400	65.840700	69.743200	73.655400
μ∗ = 0.01	57.557500	61.410500	65.246100	69.075800	72.910800
μ∗ = 0.1	53.321500	56.607000	59.845300	63.046800	66.221400
μ∗ = 1	30.815100	31.869000	32.855700	33.784300	34.662100

Table : 9 Variation of centre of pressure with respect to μ* and ε∗

σ∗= 0.05, α∗ = – 0.05, β = 1.25, a = 1.75

	ε∗ = –0.1	ε∗ = –0.05	ε∗ = 0	ε∗ = 0.05	ε∗ = 0.1
μ∗ = 0	61.244500	61.995400	62.745400	63.494500	64.242700
μ∗ = 0.001	61.186900	61.936400	62.685000	64.179300	64.179300
μ∗ = 0.01	60.673600	61.410500	62.146200	62.880800	63.614400
μ∗ = 0.1	55.981200	56.607000	57.230600	57.852100	58.471500
μ∗ = 1	31.672600	31.869000	32.062800	32.254100	32.442900

Table : 10 Variation of centre of pressure with respect to β and σ∗

ε∗ = – 0.05, a = 1.75, μ∗ = 0.001, α∗ = –0.05

	σ∗ = 0	σ∗ = 0.05	σ∗ = 0.1	σ∗ = 0.15	σ∗ = 0.2
β = 1	47.283900	47.425300	47.849300	48.555600	49.543700
β = 1.25	61.797400	61.936400	62.353400	63.048400	64.021100
β = 1.5	82.808300	82.946300	83.360500	84.050700	85.016900
β = 1.75	1.115900	1.117300	1.121400	1.128300	1.138000
β = 2	1.494700	1.496100	1.500300	1.507200	1.516800

Table :11 Variation of centre of pressure with respect to β and α∗

ε∗ = – 0.05, a = 1.75, μ∗ = 0.001, σ∗ = 0.05

	α∗ = –0.1	α∗ = –0.05	α∗ = 0	α∗ = 0.05	α∗ = 0.1
β = 1	43.516500	47.425300	51.321400	55.216800	59.123000
β = 1.25	58.018800	61.936400	65.840700	69.743200	73.655400
β = 1.5	78.993300	82.946300	86.883400	90.816100	94.755800
β = 1.75	1.077300	111.729800	1.157100	1.196800	1.236600
β = 2	1.455800	1.496100	1.536300	1.576400	161.650500

Table : 12 Variation of centre of pressure with respect to β and ε∗

σ∗ = 0.05, a = 1.75, μ∗ = 0.001, α∗ = –0.05

	ε∗ = –0.1	ε∗ = –0.05	ε∗ = 0	ε∗ = 0.05	ε∗ = 0.1
β = 1	46.646600	47.425300	48.201600	48.975800	49.748000
β = 1.25	61.186900	61.936400	62.685000	63.432600	64.179300
β = 1.5	82.214900	82.946300	83.677300	84.407900	85.138200
β = 1.75	1.1101e	1.117300	1.124500	1.131700	1.138900
β = 2	1.489000	1.496100	1.503300	1.510400	1.517600

Table : 13 Variation of centre of pressure with respect to σ∗ andα∗

μ∗ = 0.0001, ε∗ = –0.05 β = 1.25, a = 1.75

	α∗ = –0.1	α∗ = –0.05	α∗ = 0	α∗ = 0.05	α∗ = 0.1
σ∗ = 0	57.885500	61.797400	65.696000	69.592800	73.499000
σ∗ = 0.05	58.018800	61.936400	65.840700	69.743200	73.655400
σ∗ = 0.1	58.418900	62.353400	66.274800	70.194300	74.123500
σ∗ = 0.15	59.085500	63.048400	66.998000	70.946000	74.903600
σ∗ = 0.2	60.018600	64.021100	68.010400	71.998000	75.995400

Table : 14 Variation of centre of pressure with respect to σ∗ and ε∗

μ∗ = 0.0001, α∗ = – 0.05, β = 1.25, a = 1.75

	ε∗ = –0.1	ε∗ = –0.05	ε∗ = 0	ε∗ = 0.05	ε∗ = 0.1
σ∗ = 0	61.047800	61.797400	62.546000	63.293700	64.040500
σ∗ = 0.05	61.186900	61.936400	62.685000	63.432600	64.179300
σ∗ = 0.1	61.604100	62.353400	63.101800	63.849200	64.595800
σ∗ = 0.15	62.299400	63.048400	63.796400	64.543500	65.289800
σ∗ = 0.2	63.272500	64.021100	64.768700	65.515400	66.261300

Table : 15 Variation of centre of pressure with respect to α^* and ε^*

$\mu^* = 0.0001$, $\sigma^* = 0.05$, $a = 1.75$, $\beta = 1.25$

	$\varepsilon^* = -0.1$	$\varepsilon^* = -0.05$	$\varepsilon^* = 0$	$\varepsilon^* = 0.05$	$\varepsilon^* = 0.1$
$\alpha^* = -0.1$	57.270400	58.018800	58.766300	59.512700	60.258300
$\alpha^* = -0.05$	61.186900	61.936400	62.685000	63.432600	64.179300
$\alpha^* = 0$	65.090200	65.840700	66.590300	67.338900	68.086700
$\alpha^* = 0.05$	68.991800	69.743200	70.493700	71.243300	71.992000
$\alpha^* = 0.1$	72.903200	73.655400	74.406600	75.157100	75.906600

REFERENCES

[1] Marshall, P. R. and Morgan, V. T. (1965 – 66) Review of porous metal bearing development, Proc. Inst. Chem. Engrs., 180, (7), 154.
[2] Cusano, C. (1972). Lubrication of two layer porous journal bearing, Journal of Mechanical Sciences (b), 14 (5), 335 – 339.
[3] Srinivasan, U. (1977). Load capacity and time height relations for squeeze films between double layered porous plates, Wear, 43, 211 – 225.
[4] Gupta, J. L., Patel, K. C. and Hingu, J. V. (1981). An analysis of the performance of a two layer porous journal bearing, Pure and Applied Mathematical Sciences, 14 (12), 83.
[5] Bhat, M. V. and Patel, D. B. (1987). Hydrodynamic lubrication of a two layer porous slider bearing with slip velocity, National Academy of Science Letters, 10 (7), 243 – 245.
[6] Patel, K. C. and Hingu, J. V., Hydromagnetic squeeze film behavior in porous circular disks, Wear, 49, (1978). 239 – 246.
[7] Hingu, J. V. (1979). On some theoretical studies on hydrodynamic and hydromagnetic lubrication, Ph. D. Thesis, Sardar Patel University, Vallabh Vidyanagar,.
[8] Ajwaliya, M. B. (1984). On certain theoretical aspects of lubrication, Ph. D. Thesis, Sardar Patel University, Vallabh Vidyanagar,.
[9] Agrawal, V. K. (1986). Magnetic fluid based porous inclined slider bearing, Wear, 107, 133 – 139.
[10] Bhat, M. V. and Deheri, G. M. (1991). Porous composite slider bearing lubricated with magnetic fluid, Japanese Journal of Applied Physics, 30, 2513 – 2514.
[11] Bhat, M. V. and Hingu, J. V. (1978). A study of the hydromagnetic squeeze film between two layered porous rectangular plates, Wear, 50, 1 – 10.
[12] Tzeng, S. T. and Saibel, E. (1967). Surface roughness effect on slider bearing lubrication, Trans. ASME, J. Lub. Tech., 10, 334 – 338.
[13] Christensen, H. and Tonder, K. C. (1969.a). Tribology of rough surfaces: Stochastic models of hydrodynamic lubrication, SINTEF Report No. 10/69-18.
[14] Christensen, H. and Tonder, K. C. (1969.b). Tribology of rough surfaces: Parametric study and comparison of lubrication models, SINTEF Report No. 22/69-18.
[15] Christensen, H. and Tonder, K. C. (1970).Tribology of rough surfaces:A stochastic model of mixed lubrication, SINTEF Report No. 18/ 70-21.
[16] Ting, L. L. (1975). Engagement behavior of lubricated porous annular disks Part I: Squeeze film phase, surface roughness and elastic deformation effects, Wear, 34, p.p. 159 – 182.
[17] Prakash, J. and Tiwari, K. (1982). Lubrication of a porous bearing with surface corrugations, J. Lub. Tech., Trans. ASME, 104, p.p. 127 – 134.
[18] Prajapati, B.L. (1991). Behavior of squeeze film between rotating porous circular plates: Surface roughness and elastic deformation effects, Pure and Appl. Math. Sci., 33(1-2), 27 – 36.
[19] Prajapati, B.L. (1992). Squeeze film behavior between rotating porous circular plates with a concentric circular pocket: Surface roughness and elastic deformation effects, Wear, 152, 301 – 307.
[20] Guha, S. K. (1993). Analysis of dynamic characteristics of hydrodynamic journal bearings with isotropic roughness effects, Wear, 167, 173 – 179.
[21] Gupta, J. L. and Deheri, G. M. (1996),. Effect of roughness on the 1590ehavior of squeeze film in a spherical bearing, Tribology Transactions, 39, 99 – 102.
[22] Andhara, P. Gupta, J. L. and Deheri, G. M. (1999). . Effect of transverse surface roughness on the 1590ehavior of squeeze film in a spherical bearing, International Journal of Applied Mechanics and Engineering, 4, 19 – 24.

[23] Andhara, P. Gupta, J. L. and Deheri, G. M. (1997). Effect of longitudinal surface on hydrodynamic lubrication of slider bearings, Proc. Tenth International Conference on Surface Modification Technologies, The Institute on Materials,. 872 – 880.

[24] Patel, R. M., Dahari, G. and Vader, P. (2011). Magnetic fluid based squeeze film performance between porous infinitely long parallel plates with porous matrix of non-uniform thickness and effect of transverse surface roughness, Journal of Balkan Tribological Association, 17 (2),. 305 – 318.

[25] Prajapati B. L. (1995). On certain theoretical studies in hydrodynamic and electro magneto hydrodynamic lubrication. Ph. D. Thesis, S.P. University, Gujarat, India.

[26] Dahari, G., Andhara, P. and Patel, R. M. (2005). Transversely rough slider bearings with squeeze film formed by a magnetic fluid, International Journal of Applied Mechanics and Engineering, 10(1), 53 – 76.

[27] Andhara, P. I., Gupta, J. L. and Dahari, G. ., Effect of surface roughness on the hydrodynamic lubrication of slider bearings, Tribology Transaction, 44(2), (2001), 291 – 297.

[28] Lin, J. R., Hsu, C. H. and Lai, C. (2002). Surface roughness effects on the oscillating squeeze film behavior of long partial journal bearings, Computers and Structures, 80, 297 – 303.

[29] Patil, N. D. and Dahari, G. (2011). Effect of surface roughness on the performance of a magnetic fluid based parallel plates porous slider bearing with slip velocity, Journal of Serbian Society for Computational Mechanics, 5(1), 104 – 118.

[30] Patil, J. and Dahari G. (2014). Performance of a magnetic fluid based double layered rough porous slider bearing considering the combined porous structures, Acta Technica Corviniensis, Bulletin of Engineering, 7(4), 115 – 125.

[31] Patil, J. and Deheri G(2015). A comparison of different porous structures on the performance of a magnetic fluid based double porous layered rough slider bearing, International Journal of Materials Lifetime, 129 – 39.